Astron. Nachr. / AN **326**, No. 6, 409–413 (2005) / **DOI** 10.1002/asna.200510397

The stability of MHD Taylor-Couette flow with current-free spiral magnetic fields between conducting cylinders

G. RÜDIGER[1,2], R. HOLLERBACH[1,3], M. SCHULTZ[2], and D.A. SHALYBKOV[2,4]

[1] Isaac Newton Institute for Mathematical Sciences, 20 Clarkson Rd., Cambridge CB3 0EH, UK
[2] Astrophysikalisches Institut Potsdam, An der Sternwarte 16, 14482 Potsdam, Germany
[3] Department of Mathematics, University of Glasgow, Glasgow G12 8QW, UK
[4] A.F. Ioffe Institute for Physics and Technology, St. Petersburg 194021, Russia

Received 20 April 2005; accepted 25 May 2005; published online 1 July 2005

Abstract. We study the magnetorotational instability in cylindrical Taylor-Couette flow, with the (vertically unbounded) cylinders taken to be perfect conductors, and with externally imposed spiral magnetic fields. The azimuthal component of this field is generated by an axial current inside the inner cylinder, and may be slightly stronger than the axial field. We obtain an instability beyond the Rayleigh line, for Reynolds numbers of order 1000 and Hartmann numbers of order 10, and independent of the (small) magnetic Prandtl number. For experiments with $R_{\rm out} = 2\,R_{\rm in} = 10$ cm and $\Omega_{\rm out} = 0.27\,\Omega_{\rm in}$, the instability appears for liquid sodium for axial fields of $\sim$20 Gauss and axial currents of $\sim$1200 A. For gallium the numbers are $\sim$50 Gauss and $\sim$3200 A. The vertical cell size is about twice the cell size known for nonmagnetic experiments.

Key words: magnetic fields – magnetohydrodynamics – general: physical data and processes

1. Motivation

A limited number of instabilities are responsible for most of the pattern formation in the Universe. Stars are formed by the Jeans instability, and the heat transport within them is driven by the Rayleigh-Bénard instability. Most high-energy radiation, however, is produced by disks around compact objects and black holes. These accretion disks must therefore be turbulent. It is now believed that this turbulence is caused by the instability of their Keplerian rotation law in the presence of weak large-scale magnetic fields. This 'magnetorotational instability' (MRI) was first discovered by Velikhov (1959), who considered an electrically conducting fluid between rotating cylinders with $\Omega_{\rm out} < \Omega_{\rm in}$. The existence of this instability has been confirmed analytically and numerically many times; see for example Balbus (2003) and Rüdiger & Hollerbach (2004) for recent reviews.

There is considerable interest in studying the magnetorotational instability in the laboratory. The simplest, and most widely studied design, is to confine a liquid metal between differentially rotating cylinders, and impose a magnetic field along the axis of the cylinders. This yields the MRI for magnetic Reynolds numbers of order 10. However, because of the extremely small magnetic Prandtl numbers $\mathrm{Pm}(=\nu/\eta)$ of available liquid metals (see Table 1), that translates into ordinary Reynolds numbers exceeding 10^6, which causes severe difficulties (Hollerbach & Fournier 2004). In order to overcome such problems, Hollerbach & Rüdiger (2005) proposed imposing an azimuthal field as well, with dramatic consequences, namely a reduction of the critical Reynolds number $\mathrm{Re_c}$ from $O(10^6)$ to $O(10^3)$. These new solutions are also essentially independent of Pm, and are therefore ideally suited to experimental realisations in the laboratory. These results were for insulating inner and outer cylinders, in which case the axial current one must impose to generate this azimuthal magnetic field is around 2500 A (using liquid sodium as the fluid), which is close to the upper limit of what is experimentally possible. Here we therefore consider conducting cylinders, and show that the necessary current (as well as the Reynolds number) is smaller than for insulating cylinders.

Correspondence to: gruediger@aip.de

Table 1. Liquid metal material parameters in c.g.s.

	ρ	ν	η	Pm	$\sqrt{4\pi\rho\nu\eta}$
sodium	0.9	$7.1\cdot10^{-3}$	$0.8\cdot10^{3}$	$0.9\cdot10^{-5}$	8.15
gallium	6.0	$3.2\cdot10^{-3}$	$2.1\cdot10^{3}$	$1.5\cdot10^{-6}$	22.0

2. Introduction

We consider the stability of the flow between two rotating coaxial infinitely long cylinders, in the presence of a constant axial field B_z, and a current-free (within the fluid) azimuthal field B_ϕ. Figure 1 shows a sketch of the geometry. The fluid is incompressible, with density ρ, kinematic viscosity ν and magnetic diffusivity η.

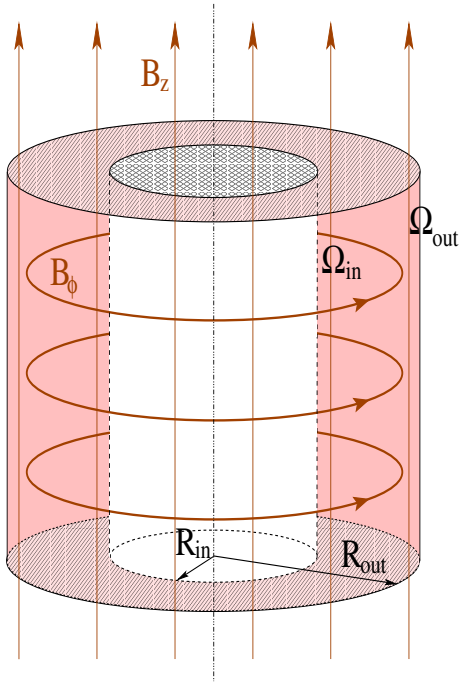

Fig. 1. (online colour at www.an-journal.org) The basic geometry of the problem, consisting of two cylinders of radii $R_{\rm in}$ and $R_{\rm out}$, rotating at $\Omega_{\rm in}$ and $\Omega_{\rm out}$. B_z and B_ϕ are the externally imposed magnetic fields, B_ϕ by an axial current inside the inner cylinder.

By conservation of angular momentum the basic state differential rotation profile is given by

$$\Omega = a + \frac{b}{R^2}, \tag{1}$$

where a and b are given by

$$a = \frac{\hat{\mu} - \hat{\eta}^2}{1-\hat{\eta}^2}\Omega_{\rm in}, \qquad b = \frac{1-\hat{\mu}}{1-\hat{\eta}^2}R_{\rm in}^2\Omega_{\rm in}, \tag{2}$$

with $\hat{\mu} = \Omega_{\rm out}/\Omega_{\rm in}$ and $\hat{\eta} = R_{\rm in}/R_{\rm out}$. $R_{\rm in}$ and $R_{\rm out}$ are the radii of the inner and outer cylinders, and $\Omega_{\rm in}$ and $\Omega_{\rm out}$ are their angular velocities.

From the azimuthal component of the induction equation one finds

$$B_\phi = \frac{B}{R} \tag{3}$$

with $B = \beta B_0 R_{\rm in}$. This parameter β therefore denotes the ratio of the toroidal field to the constant axial field $B_z = B_0$. This toroidal field B_ϕ is maintained by an electric current running along the central axis of strength

$$J = 5\beta B_0 R_{\rm in} \tag{4}$$

with J in Ampere, B_0 in Gauss and $R_{\rm in}$ in cm.

We are interested in the stability of the basic state (1) against axisymmetric and nonaxisymmetric perturbations. The perturbed state of the flow is described by the quantities

$$u_R', \;\; R\Omega + u_\phi', \;\; u_z', \;\; B_R', \;\; B_\phi + B_\phi', \;\; B_0 + B_z'. \tag{5}$$

The solutions of the linearized MHD equations are considered in their modal representation $\boldsymbol{F}' = \boldsymbol{F}'(R)\exp(\mathrm{i}(kz + m\phi + \omega t))$ where $\boldsymbol{F}'$ is any of $\boldsymbol{u}'$ and $\boldsymbol{B}'$. The dimensionless numbers of the problem are the magnetic Prandtl number Pm, the Hartmann number Ha and the Reynolds number Re,

$$\mathrm{Pm} = \frac{\nu}{\eta}, \quad \mathrm{Ha} = \frac{B_0 R_0}{\sqrt{\mu_0 \rho \nu \eta}}, \quad \mathrm{Re} = \frac{\Omega_{\rm in} R_0^2}{\nu}, \tag{6}$$

where μ_0 is the permeability, and $R_0 = (R_{\rm in}D)^{1/2}$ with $D = R_{\rm out} - R_{\rm in}$.

In order to understand the results presented here, it is useful also to consider the induction equation for the fluctuating toroidal field component,

$$\frac{\partial B_\phi'}{\partial t} - \eta \Delta B_\phi' = \mathrm{rot}_\phi\left(\bar{\boldsymbol{u}}_\phi \times \boldsymbol{B}_{\rm pol}' + \boldsymbol{u}_\phi' \times \bar{\boldsymbol{B}}_{\rm pol} + \boldsymbol{u}_{\rm pol}' \times \bar{\boldsymbol{B}}_\phi\right) \tag{7}$$

where $\boldsymbol{u}_{\rm pol}$ and $\boldsymbol{B}_{\rm pol}$ denote the poloidal components of $\boldsymbol{u}$ and $\boldsymbol{B}$. Chandrasekhar (1961) cancelled the last two terms on the right of this equation, and did not obtain the MRI. It occurs if only the last term in (7) is cancelled; but one can show that for small Pm it only appears for $\mathrm{Rm} = O(10)$. If also the last term in (7) is retained then the resulting Reynolds number loses its strong $\mathrm{Re} \propto \mathrm{Pm}^{-1}$ dependence, and is reduced by 3 orders of magnitude (Hollerbach & Rüdiger 2005, see also Table 4).

3. The equations

The equations of the problem are given in a similar form as by Rüdiger & Shalybkov (2004). Lengths and wave numbers are normalized by R_0, velocities by η/R_0, frequencies by $\Omega_{\rm in}$, and magnetic fields by B_0. One then obtains

$$\frac{\mathrm{d}P'}{\mathrm{d}R} + \mathrm{i}\frac{m}{R}X_2 + \mathrm{i}kX_3 + \left(k^2 + \frac{m^2}{R^2}\right)u_R' + \\ + \mathrm{iRe}(\omega + m\Omega)u_R' - 2\Omega\,\mathrm{Re}\,u_\phi' - \mathrm{iHa}^2 k B_R' - \\ - \mathrm{iHa}^2\frac{mB}{R^2}B_R' + 2\mathrm{Ha}^2\frac{B}{R^2}B_\phi' = 0, \tag{8}$$

$$\frac{\mathrm{d}X_2}{\mathrm{d}R} - \left(k^2 + \frac{m^2}{R^2}\right)u_\phi' - \mathrm{iRe}(\omega + m\Omega)u_\phi' + 2\mathrm{i}\frac{m}{R^2}u_R' - \\ - 2\mathrm{Re}\,a\,u_R' + \mathrm{iHa}^2\frac{mB}{R^2}B_\phi' + \mathrm{iHa}^2 k B_\phi' - \mathrm{i}\frac{m}{R}P' = 0, \tag{9}$$

$$\frac{\mathrm{d}X_3}{\mathrm{d}R} + \frac{X_3}{R} - \left(k^2 + \frac{m^2}{R^2}\right)u_z' - \mathrm{iRe}(\omega + m\Omega)u_z' - \\ - \mathrm{i}kP' + \mathrm{iHa}^2\frac{mB}{R^2}B_z' + \mathrm{iHa}^2 k B_z' = 0, \tag{10}$$

$$\frac{\mathrm{d}u_R'}{\mathrm{d}R} + \frac{u_R'}{R} + \mathrm{i}\frac{m}{R}u_\phi' + \mathrm{i}ku_z' = 0, \tag{11}$$

$$\frac{\mathrm{d}B_z'}{\mathrm{d}R} - \frac{\mathrm{i}}{k}\left(k^2 + \frac{m^2}{R^2}\right)B_R' + \mathrm{Pm}\,\mathrm{Re}\frac{(\omega + m\Omega)}{k}B_R' + \\ + \frac{m}{kR}X_4 - \frac{m}{kR}b\,u_R' - u_R' = 0, \tag{12}$$

$$\frac{\mathrm{d}X_4}{\mathrm{d}R} - \left(k^2 + \frac{m^2}{R^2}\right) B'_\phi - \mathrm{i}\mathrm{Pm}\,\mathrm{Re}(\omega + m\Omega)B'_\phi + \\ + \mathrm{i}\frac{2m}{R^2}B'_R + 2\frac{B}{R^2}u'_R - 2\mathrm{Pm}\,\mathrm{Re}\frac{b}{R^2}B'_R + \\ + \mathrm{i}\frac{mB}{R^2}u'_\phi + \mathrm{i}k\,u'_\phi = 0, \quad (13)$$

$$\frac{\mathrm{d}B'_R}{\mathrm{d}R} + \frac{B'_R}{R} + \mathrm{i}\frac{m}{R}B'_\phi + \mathrm{i}kB'_z = 0 \quad (14)$$

with P' as the pressure and

$$X_2 = \frac{u'_\phi}{R} + \frac{\mathrm{d}u'_\phi}{\mathrm{d}R},\ X_3 = \frac{\mathrm{d}u'_z}{\mathrm{d}R},\ X_4 = \frac{B'_\phi}{R} + \frac{\mathrm{d}B'_\phi}{\mathrm{d}R}. \quad (15)$$

The boundary conditions for the flow are $u'_R = u'_\phi = u'_z = 0$ for $R = R_{\rm in}$ and $R = R_{\rm out}$. The boundary conditions for the magnetic field are also straightforward; taking the inner and outer cylinders to be perfectly conducting, they are simply $B'_R = 0$, $X_4 = 0$ for $R = R_{\rm in}$ and $R = R_{\rm out}$. We will consider only the particular radius ratio $\hat{\eta} = 0.5$.

4. Axisymmetric modes

Figure 2 shows the critical Reynolds numbers at and beyond the Rayleigh line for experiments without toroidal magnetic fields, the classical design. We note how $\mathrm{Re_c}$ jumps abruptly from 10^4 to 10^6 (for liquid sodium, see Rüdiger, Schultz & Shalybkov 2003). With a toroidal field, however, the solutions are very different, as shown in Fig. 3. The toroidal field strongly modifies the extremely steep line obtained for $\beta = 0$ (Fig. 2). Its inclination is reduced and it starts at lower Reynolds numbers. For $\beta \gtrsim 2$ we find critical Reynolds numbers of order 10^3. This is a dramatic reduction of the values of order 10^6 which are characteristic for $\beta = 0$.

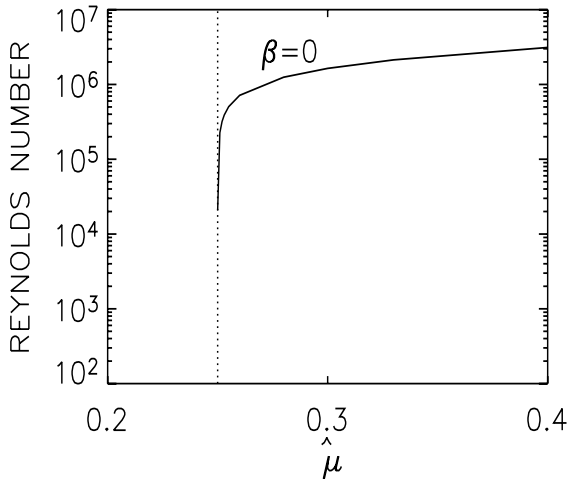

Fig. 2. On the Rayleigh line (here $\hat{\mu} = 0.25$, dotted line) the critical Reynolds number scales as $\mathrm{Pm}^{-0.5}$, while beyond the Rayleigh line it scales as Pm^{-1}, so that for $\mathrm{Pm} = 10^{-5}$ the critical Reynolds number jumps from 10^4 to 10^6.

The corresponding Hartmann numbers for these instabilities are also strongly reduced by the inclusion of a toroidal field (Fig. 4). Tables 2 and 3 show results for $\hat{\mu} = 0.27$, $\beta = 0$ to 4, and $\mathrm{Pm} = 10^{-5}$ (sodium, Table 2) and $\mathrm{Pm} = 10^{-6}$ (gallium, Table 3). The first five columns show the nondimensional quantities indicated. The last four columns show dimensional quantities, taking $R_{\rm in} = 5$ cm and $R_{\rm out} = 10$ cm. Specifically, Re has been converted to $f_{\rm in}$, the rotation frequency, in Hz, of the inner cylinder. The Hartmann number Ha has been converted first to B_0, the strength, in Gauss, of the axial field. Next, the product β Ha has been converted to the strength of the azimuthal field at $R_{\rm in}$. Finally, J denotes the axial current, in Ampere, that is required to maintain this toroidal field.

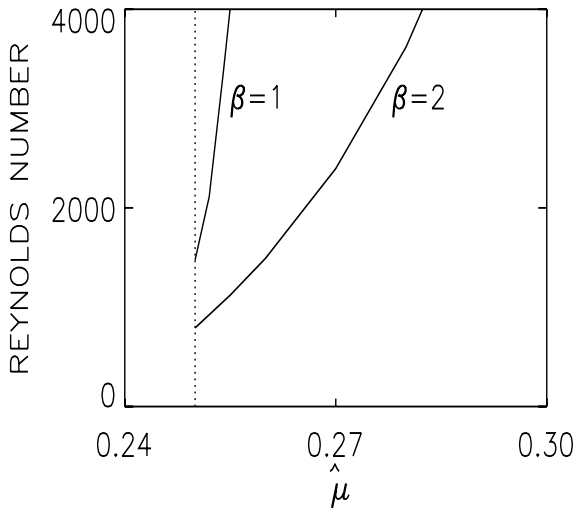

Fig. 3. The critical Reynolds numbers beyond the Rayleigh line, for axisymmetric modes ($m = 0$) with toroidal fields of the same order of magnitude as the axial field. $\mathrm{Pm} = 10^{-5}$.

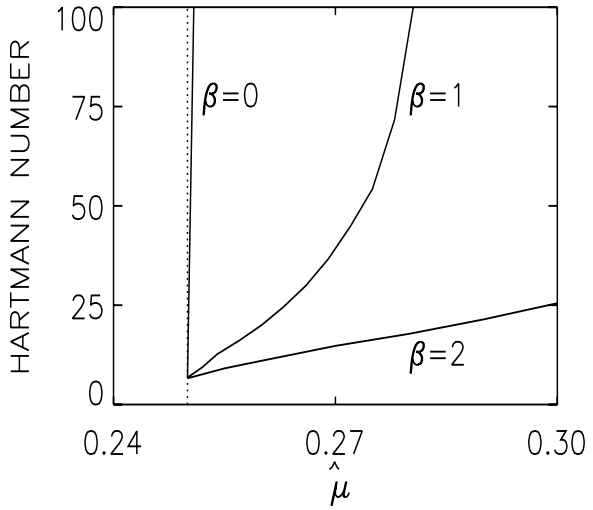

Fig. 4. The Hartmann numbers of the solutions given in Fig. 3.

For $\beta \gtrsim 2$ we see then that the critical Reynolds numbers no longer scale as Pm^{-1}, as they do for $\beta = 0$, but rather become independent of Pm. This is the same result previously noted by Hollerbach & Rüdiger (2005) for insulating boundaries. More quantitatively, we note that for $\beta \gtrsim 2$ the required rotation rates of the inner cylinder are reduced to less than 1

Table 2. Characteristic values for $\hat{\eta} = 0.5$, $\hat{\mu} = 0.27$, and $\mathrm{Pm} = 10^{-5}$. In converting from nondimensional to dimensional quantities $R_{\rm in} = 5$ cm and $R_{\rm out} = 10$ cm were used, and the material properties of sodium. The magnetic fields are measured in Gauss, B_ϕ denotes the toroidal field at the inner cylinder, the current J is measured in Ampere. $\Re(\omega)$ is the real part of the Fourier frequency.

β	Re	Ha	k	$\Re(\omega)$	$f_{\rm in}$	B_0	B_ϕ	J
0	$1 \cdot 10^6$	542	1.7	0	45	883	0	0
1	33833	38.4	0.6	0.04	1.5	63	63	1565
2	2383	14.6	1.3	0.10	0.11	24	48	1190
3	1160	10.7	1.6	0.13	0.05	17	52	1308
4	842	9.5	2.0	0.15	0.04	15	62	1549

Table 3. The same as in Table 2 but for gallium ($\mathrm{Pm} = 10^{-6}$).

β	Re	Ha	k	$\Re(\omega)$	$f_{\rm in}$	B_0	B_ϕ	J
0	$1 \cdot 10^7$	1720	1.7	0	200	7568	0	0
1	38250	39	0.6	0.04	0.8	171	171	4290
2	2382	14.6	1.3	0.10	0.05	64	128	3212
3	1160	10.8	1.7	0.13	0.02	48	143	3564
4	842	9.5	2.0	0.15	0.02	42	167	4180

Hz, the axial fields to a few tens of Gauss, and the axial currents to $O(1000)$ A. All of these values are easily achievable in the laboratory. We conclude therefore that this new design, incorporating an axial current, is the most promising design for obtaining the MRI in a laboratory experiment.

It is important also to consider the wave numbers k; if the vertical cell size is too large the experiment will still run into difficulties. We note in Fig. 5 that for non-zero β k is reduced somewhat, corresponding to a greater extent in z (the vertical cell size is given by $\delta z \approx \pi/k$). The increase in cell size is not very great though, and therefore should not cause any problems.

Another interesting point in comparing k for $\beta = 0$ versus $\beta > 0$ is the Pm-dependence, or rather the lack thereof, since k is independent of Pm in both cases. The details of how this comes about are subtly different though. For the classical MRI with $\beta = 0$ the critical wave number is proportional to $\Omega_{\rm in}/V_{\rm A}$, where $V_{\rm A} = B_0/\sqrt{\mu_0 \rho}$ is the Alfvén velocity. The nondimensional wave number k then becomes

$$k \propto \frac{\mathrm{Re}\sqrt{\mathrm{Pm}}}{\mathrm{Ha}}, \tag{16}$$

which does *not* depend on the magnetic Prandtl number, since $\mathrm{Re} \propto \mathrm{Pm}^{-1}$ and $\mathrm{Ha} \propto \mathrm{Pm}^{-1/2}$. In contrast, for $\beta > 0$ k is still independent of Pm, but so are Re and Ha, so that (16) cannot be the relevant balance in this case. For $\beta > 0$ the actual wave numbers are much greater than (16) would predict.

Finally, Fig. 6 shows the frequency $\Re(\omega)$ of these modes. For $\beta = 0$ this is zero, since the modes are stationary in that case. For non-zero β stationary modes no longer exist; as noted also by Hollerbach & Rüdiger (2005), including a toroidal field changes the symmetries of the problem in such a way that $\pm z$ are no longer equivalent, which inevitably means that the modes will drift one way or the other in z, that is, they will be oscillatory rather than stationary. We see though that the real parts of ω are still rather small, with the mode-oscillation time exceeding the rotation time of the inner cylinder by more than a factor of 10.

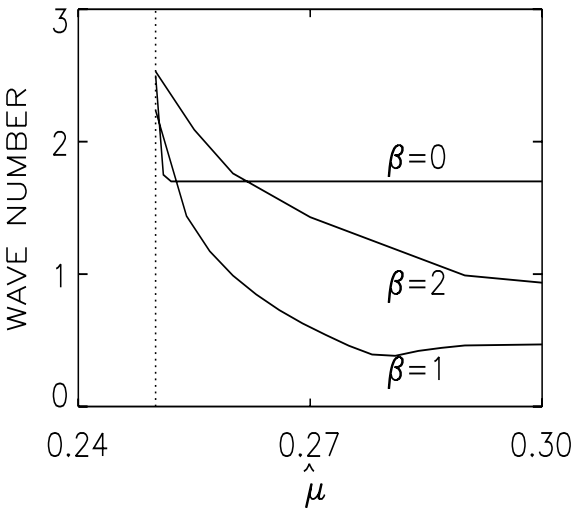

Fig. 5. The wave numbers k of the solutions given in Fig. 3.

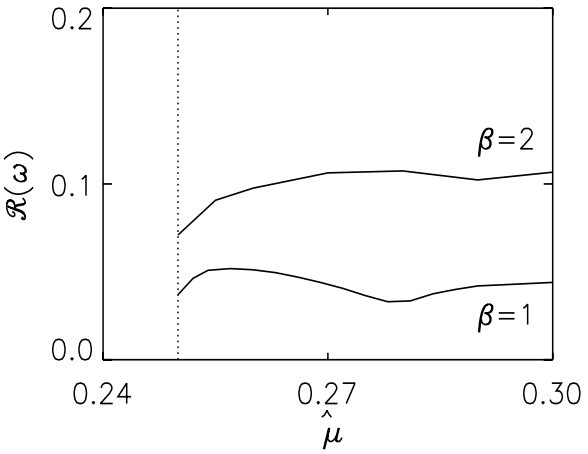

Fig. 6. The real parts of the eigenfrequency ω of the solutions given in Fig. 3.

Table 4. Insulating cylinders: Fields and axial current for $\hat{\eta} = 0.27$ and $\beta = 4$ ($R_{\rm in} = 5$ cm, $R_{\rm out} = 10$ cm). The magnetic fields are measured in Gauss, B_ϕ denotes the toroidal field at the inner cylinder, the current J is measured in Ampere.

	Re	$f_{\rm in}$ [Hz]	Ha	B_z	B_ϕ	J
sodium	1521	0.07	16.3	26	106	2657
gallium	1521	0.03	16.3	72	287	7170

5. Nonaxisymmetric modes

Hollerbach & Rüdiger considered only axisymmetric modes $m = 0$. These are usually the preferred modes, both in nonmagnetic Taylor-Couette flow, as well as in the classical $\beta = 0$ MRI. Nevertheless, for a complete analysis the nonaxisymmetric modes with $m > 0$ must also be considered. Figure 7 shows these results, and demonstrates that here too the critical Reynolds numbers for the onset of nonaxisymmetric modes are greater than for the onset of axisymmetric modes. Indeed, including a toroidal field reduces $\mathrm{Re_c}$ by far less for the nonaxisymmetric than for the axisymmetric modes. For $\beta \gtrsim 1$ the axisymmetric modes thus occur several orders of magnitude before the nonaxisymmetric ones do. These nonaxisymmetric modes are therefore not interesting from the point of view of doing laboratory experiments.

6. Conclusion

The central conclusion of this work is as before in Hollerbach & Rüdiger (2005), that imposing both axial and azimuthal magnetic fields together dramatically reduces the critical Reynolds numbers required to obtain the magnetorotational instability. However, for the insulating boundary conditions considered there, the axial currents required to generate this new toroidal field were at the upper range of what could be achieved in the lab. Here we therefore considered conducting cylinders, and found that the required currents (and Reynolds numbers) are smaller. For comparison, Table 4 presents the results of Hollerbach & Rüdiger for $\beta = 4$; we see that $\mathrm{Re} = 1521$ and $\mathrm{Ha} = 16.3$, compared with $\mathrm{Re} = 842$ and $\mathrm{Ha} = 9.5$ here (the last rows of Tables 2 and 3). Switching from insulating to conducting boundaries thus reduces both Re and Ha by almost a factor of 2, which would certainly help in achieving these toroidal fields in the lab. We conclude therefore that implementing this experiment with conducting boundaries is the most promising design for exploring the magnetorotational instability in the laboratory.

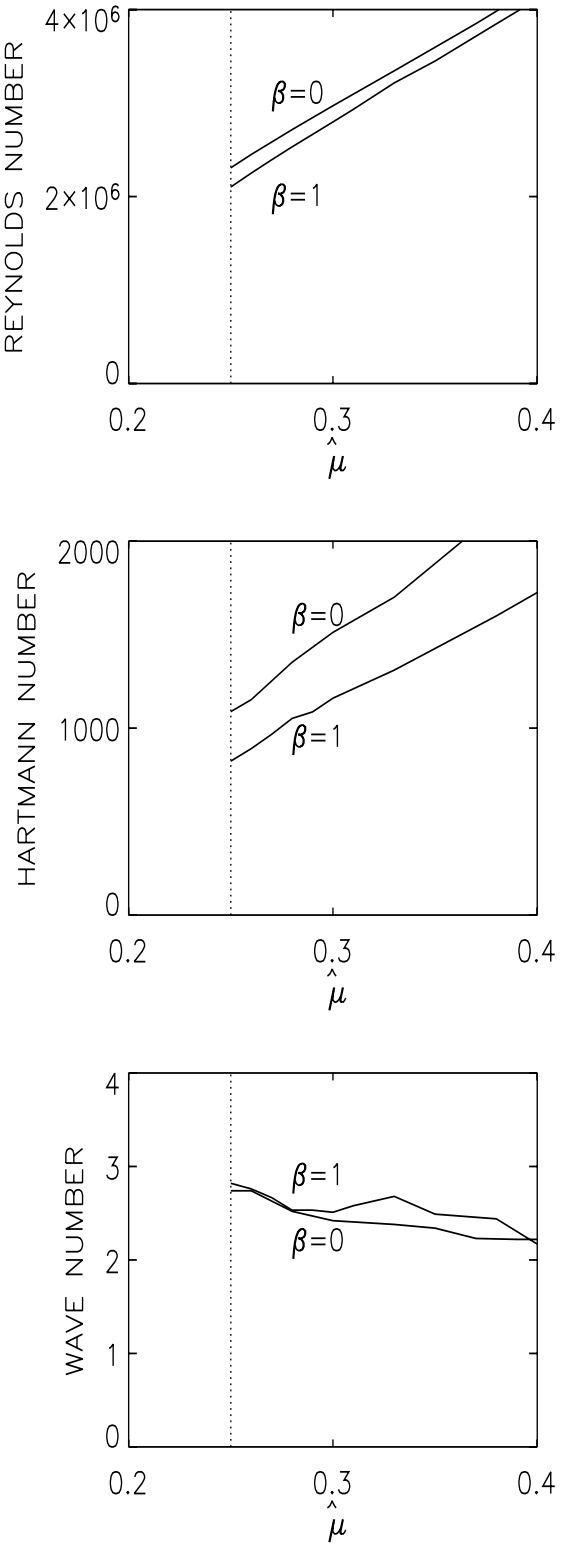

Fig. 7. Critical Reynolds numbers (top), Hartmann numbers (middle) and wave numbers (bottom) for nonaxisymmetric modes with $m = 1$.

References

Balbus, S.A.: 2003, ARA&A 41, 555
Chandrasekhar, S.: 1961, *Hydrodynamic and Hydromagnetic Stability*, Oxford University Press
Hollerbach, R., Fournier, A.: 2004, in: R. Rosner, G. Rüdiger, A. Bonanno (eds.), *MHD Couette Flows: Experiments and Models*, AIP Conf. Proc. 733, 114
Hollerbach, R., Rüdiger, G.: 2005, PhRvL, submitted
Rüdiger, G., Schultz, M., Shalybkov, D.A.: 2003, PhRvE 67, 046312
Rüdiger, G., Hollerbach, R.: 2004, *The Magnetic Universe: Geophysical and Astrophysical Dynamo Theory*, Wiley-VCH, Berlin
Rüdiger, G., Shalybkov, D.A.: 2004, PhRvE 69, 016303
Velikhov, E.P.: 1959, SJETP 9, 995